Curvature Angle Splitting Suppression and Optimization on Nonplanar Coils Used in Wireless Charging System

Feng Wen, Fansheng Jing, Qiang Li, Rui Li, Li Liu, and Xiaohu Chu

***Abstract*—This article investigates the tapered and curved coil used in wireless power transfer (WPT) system for the purpose of improving flexibility in specific applications. The WPT transmission performance is always declined by coil bending. To solve this problem, the models of the coils are built, and their magnetic flux are analyzed. The phenomenon of curvature angle splitting is studied, the mechanism is revealed, and the method is proposed to avoid the splitting. Formulas are derived to determine whether the system is working in curvature angle splitting state. By optimizing the coil parameters to make the system work in critical splitting state, the maximum output power and excellent stability under different angles are achieved. Experimental results show that when the optimally designed receiver coil is bent in the range of 50°–130°, the maximum current change rate is only 4.3%. The study in this article will further promote the application of WPT technology in a wider range of fields.**

***Index Terms*—Angle splitting, curved coil, power stabilization, tapered coil, wireless power transfer (WPT).**

I. Introduction

With the application of wireless power transfer (WPT) technology, in order to promote system transmission performance in different application scenarios, scholars at worldwide have developed a variety of topological structures. From the initial two-coil coupled structure, three coils [1] and four coils [2] with relay links have gradually evolved, and the winding forms have also become various, such as space spiral type [3], flat disk type, and double-D type [4]. The development of WPT technology has also promoted the transformation of military equipment worldwide, such as wireless charging system for military sensor network [5], digital soldier and vehicle wireless charging system [6], underwater WPT system [7], and ground rocket power supply system. Wireless power supply system used in military fields, such as missiles and rockets [8], can use nonplanar coils to fit conical or cylindrical structures, which is convenient for system installation and fixation. At present, relevant research works have been carried out on the optimization of coil parameters and the application of curved coils in WPT system at home and abroad. Literatures [9]–[11] use flexible printed circuit board (PCB) receiver coil and cooperate with strap bending to adapt to curvature of wrist. In specific, the electrical parameters of flexible coil with the change of curvature radius are analyzed, and the experimental results show that power transmission efficiency between two coils can also reach about 50%. However, the transmission power is unstable due to the impact of wrist movement and curvature changes when wearing. In [12] and [13], the influence of RFID tag coil bending on radio frequency identification performance is studied. The coil bending causes inductive coupling between reader and electronic tag to decrease, and RF reading range is reduced; by increasing inductance of curved coil, it is ensured that there is proper inductance coupling when it is bent [14]. Since the working principle of wireless power transmission and radio frequency communication is not the same, this method can provide reference for the application of curved coil in WPT. The performance of WPT system using a curved relay resonator to extend transmission distance has been studied in [15]. Experiments have shown that using a curved relay coil can effectively extend the wireless power transmission distance. However, as coil curvature increases, the wireless transmission power (especially the maximum received power) will decrease. Based on current research works on curved coil by scholars all over the world, it can be found that the popularization and application of curved coil still face problems, such as reduced system transmission power caused by coil bending and transmission power fluctuations caused by coil curvature changing.

In the WPT system for military equipment, the planar circular coil does not fit the equipment surface very well in some applications. As shown in Fig. 1, by dragging and bending, the planar coil can be reconstituted into a tapered coil that fit the truncated taper and a curved coil that fit the cylinder, as shown in Type-I and Type-II in Fig. 1. These nonplanar coils can be applied to rocket fairings, arrows, space shuttle booster cones, missile cones, and missile bodies. Therefore, this article

Manuscript received October 16, 2019; revised December 28, 2019 and January 21, 2020; accepted February 13, 2020. Date of publication February 17, 2020; date of current version May 1, 2020. This work was supported in part by the Basic Research Program of Jiangsu Province under Grant BK20180485, in part Jiangsu Provincial Key Laboratory of Smart Grid Technology and Equipment Project, and in part the Fundamental Research Funds for the Central Universities under Grant 30919011241. Recommended for publication by Associate Editor M. Ponce-Silva. *(Corresponding author: Feng Wen.)*

Feng Wen is with the Department of Electrical Engineering, School of Automation, Nanjing University of Science and Technology, Nanjing 210094, China, and also with the Jiangsu Provincial Key Laboratory of Smart Grid Technology and Equipment, Nanjing 210096, China (e-mail: wen@njust.edu.cn).

Fansheng Jing, Qiang Li, Rui Li, Li Liu, and Xiaohu Chu are with the Department of Electrical Engineering, School of Automation, Nanjing University of Science and Technology, Nanjing 210094, China (e-mail: jingly@njust.edu.cn; chnliqiang@njust.edu.cn; 117110011042@njust.edu.cn; 117110022146@njust.edu.cn; chu@njust.edu.cn).

Color versions of one or more of the figures in this article are available online at http://ieeexplore.ieee.org.

Digital Object Identifier 10.1109/TPEL.2020.2974619

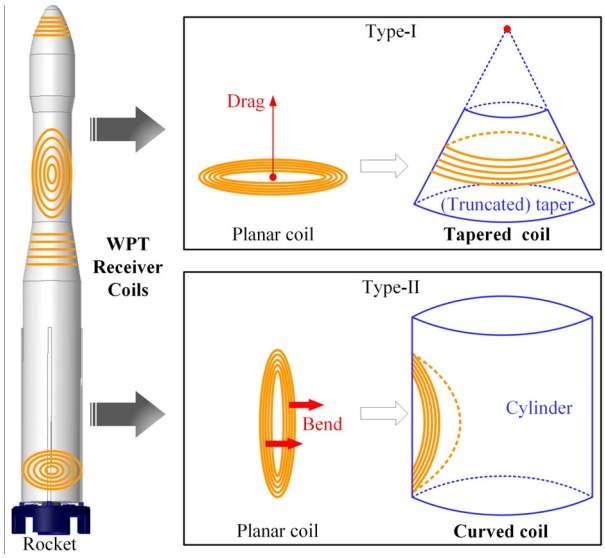

Fig. 1. Reconstruction of planar coils.

proposes to use tapered coil and curved coil as a receiver coil of the WPT system, which can fully fit the equipment surface, improve the overall design of military equipment, and promote more in-depth application of WPT technology to military field.

According to the structural characteristics of military equipment, such as rockets and missiles, this article proposes the use of tapered coils and curved coils as receivers in the WPT system. Different application fields are studied by changing the curvature of receiver coils, and the best performance of the WPT system when curvature angle changes is also explored. This article conducts research by system modeling, analysis optimization, and experimental verification. In Section II system modeling is presented, which performs equivalent modeling analysis and magnetic field calculations on tapered and curved coil, respectively. Section III analyzes and optimizes the tapered coil (Type-I), explores the influence of the coil inner diameter and the turn spacing on the angle splitting and the transmission performance of the system under different transmission distances, and then summarizes the design method of the system parameters. Section IV focuses on the analysis and optimization of curved coil (Type-II), studies the mechanism of curvature angle splitting and corresponding suppression methods, and then summarizes the relationship between the magnetic flux and the receiver coil parameters, the relationship between the magnetic flux change rate, the transmission distance, and the receiver coil parameters. Section V presents the experimental verification, the experimental analysis of the relationship between the magnetic flux change rate and the transmission distance, and the critical splitting of the curvature angle and the system power stability. This article provides a useful reference for the application of nonplanar coils in the WPT system and promotes its applicability in more occasions.

II. System Modeling and Magnetic Field Calculation

In this section, the proposed tapered coil and curved coil are modeled and analyzed, and system's magnetic field calculation is performed, which provides theoretical support for the later study of the relationship between transmission performance and coil parameters. The parameters of tapered coil and curved coil are shown in Table I.

TABLE I
Nonplanar Coils Parameter Symbol

Parameter symbol	Tapered coil	Curved coil
Inner diameter	$2r_{1T}$	$2r_{1C}$
Outer diameter	$2r_{2T}$	$2r_{2C}$
Turn spacing	d_{2T}	d_{2C}
Number of turns	n_{2T}	n_{2C}
Curvature angle	θ_T	θ_C
Transmission distance	h_{exT}	h_{exC}

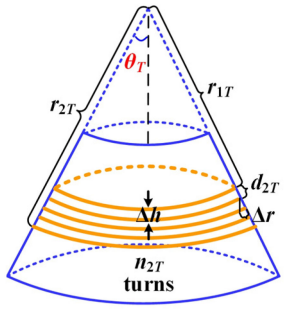

Fig. 2. Model of a tapered coil.

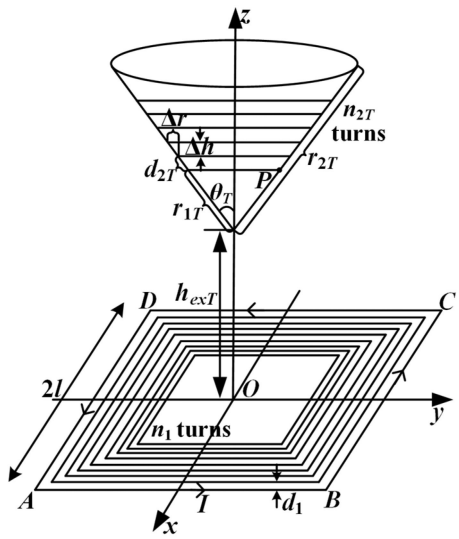

Fig. 3. Simplified model of the tapered coil WPT system.

A. Magnetic Field Calculation of Tapered Coil: Type-I

A simplified model of tapered coil is shown in Fig. 2. The angle between side of cone and the axis is θ_T, the distance between turns on tapered surface is d_{2T}, the height difference between turns is $\Delta h = d_{2T}\cos\theta_T$, the coil radius difference $\Delta r = d_{2T}\sin\theta_T$, and the distance from the vertex of cone to the nearest and furthest turn is r_{1T} and $r_{2T}=r_{1T} + (n_{2T} - 1)\, d_{2T}$, respectively.

Fig. 3 shows a simplified model of tapered coil WPT system. The transmitter coil adopts a flat square structure with a side length of $2l$, a number of turns of n_1, a turn spacing of d_1, and a side length of the innermost square coil of $2l-2(n_1-1)d_1$; set the current flow direction to be counterclockwise, and the size to be I. Taking the center of the transmitter coil as the origin O, and the plane on which it is located is *xoy* plane, the coordinate system shown in Fig. 3 is established. The tapered receiver coil is coaxial with the transmitter coil, and the height from its vertex to transmitter coil is h_{exT}.

Take a point P on the innermost side of the tapered receiver coil, and set the coordinate of point P as (0, $r_{1T}\sin\theta_T$, $h_{exT}+r_{1T}\cos\theta_T$). Since the magnetic induction intensity on a circumference of same radius is equal, according to the Biot–Savart law [16], [17], the magnetic field generated by a current-carrying straight wire at a certain point in space can be calculated by the following formula:

$$B=\frac{\mu_0 I}{4\pi a}(\cos\theta_1-\cos\theta_2) \tag{1}$$

where a is the vertical distance from a certain point in the space to the current carrying straight wire; θ_1 is the angle between the line from desired point to current inflow point and the current flow direction; θ_2 is the angle between the line connecting desired point to the current outflow point and the current flow direction; I is the current flowing through straight wire; and μ_0 is the vacuum permeability, and its value is $4\pi\times10^{-7}$. By superimposing the n_1 turns of the transmitter coil, the magnitude of magnetic field generated by the entire transmitter coil along the x-axis, y-axis, and z-axis at point P in space can be deduced, that is

$$\begin{cases} B_x=\sum_{i=1}^{n_1}(B_{BCxi}+B_{DAxi}+B_{CDxi}+B_{ABxi}) \\ B_y=\sum_{i=1}^{n_1}(B_{BCyi}+B_{DAyi}+B_{CDyi}+B_{AByi}) \\ B_z=\sum_{i=1}^{n_1}(B_{BCzi}+B_{DAzi}+B_{CDzi}+B_{ABzi}). \end{cases} \tag{2}$$

The magnetic induction lines along the x- and y-axis directions are parallel to the tapered coil, so only the magnetic field component B_z in the z-axis direction needs to be considered in the calculation. By the formula $d\Phi=B\times dS$, the magnetic induction intensity B_z can be integrated in a circular area with a radius of $r_{1T}\sin\theta_T$ [18], and the magnetic flux passing through the innermost turns of the receiver coil can be calculated as formula (3); it should be noted here that the vertical distance from the innermost turn of the tapered coil to the transmitter coil is $h_{exT}+r_{1T}\cos\theta_T$

$$\begin{aligned}\Phi_{S1}&=\int d\Phi=\int B_z\cdot ds \\ &=\int_0^{r_{1T}\sin\theta_T} B_z(h_{exT}+r_{1T}\cos\theta_T)\cdot 2\pi r\cdot dr.\end{aligned} \tag{3}$$

According to formula (3) and the magnetic linkage calculation formula $\Psi=N\Phi$, the magnetic flux linkage expression passing through the tapered receiver coil can be superimposed,

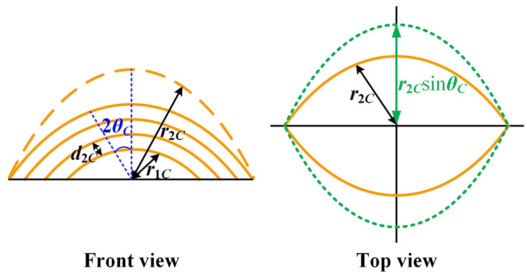

Fig. 4. Equivalent of the curved coil.

that is

$$\begin{aligned}\Psi_{(Ta)}&=\Phi_{s1}+\Phi_{s2}+\cdots+\Phi_{sn_2} \\ &=\sum_{j=1}^{n_{2T}}\sum_{i=1}^{n_1}\int_0^{R(j)}2\pi r\left\{\frac{\mu IL(i)B(r)}{2\pi\sqrt{A(i)+B(r)^2}}\cdot D(r)\right. \\ &\quad\left.+\frac{\mu IL(i)C(r)}{2\pi\sqrt{A(i)+C(r)^2}}\cdot E(r)\right\}dr\end{aligned}$$

$$\begin{cases} h=h_{exT}+r_{1T}\cos\theta_T+(j-1)d_{2T}\cos\theta_T \\ R(j)=r_{1T}\sin\theta_T+(j-1)d_{2T}\sin\theta_T \\ L(i)=l-(i-1)d_1 \\ A(i)=L(i)^2+h^2 \\ B(r)=L(i)-r \\ C(r)=L(i)+r \\ D(r)=\frac{1}{h^2+[L(i)-r]^2}+\frac{1}{h^2+L(i)^2} \\ E(r)=\frac{1}{h^2+[L(i)+r]^2}+\frac{1}{h^2+L(i)^2} \end{cases}$$

$$\text{s.t. } l-(n_1-1)d_1>0. \tag{4}$$

B. Equivalent and Calculation of Curved Coil: Type-II

To simplify the calculation, the curved receiver coil is equivalent to a planar coil, as shown in Fig. 4. The straight line distance from curved coil's center to the outermost turn is r_{2C}, the line distance from the center of curved coil to the innermost turn is r_{1C}, and the turn spacing is d_{2C}. Project curved coil to the bottom surface, and get an equivalent coil, which is approximately circular; the angle between two straight lines from the center of the curved coil to the outermost turns on both sides is $2\theta_C$, with θ_C being the curvature angle, which reflects the degree of bending of coil. The number of turns of both the equivalent coil and the original coil is n_{2C}, and the outer diameter, inner diameter, and turn spacing of equivalent coil are $2r_{2C}\sin\theta_C$, $2r_{1C}\sin\theta_C$, and $d_{2C}\sin\theta_C$; when the coil bending degree is small, equivalent error can be ignored.

Fig. 5 shows a simplified model of a curved coil WPT system. The transmitter coil adopts the same structure and size as the tapered coil WPT system. According to the abovementioned analysis, when the coil bending degree is small, the influence of curved coil bending on the transmission distance can be ignored. At this time, the magnetic flux expression of the tapered

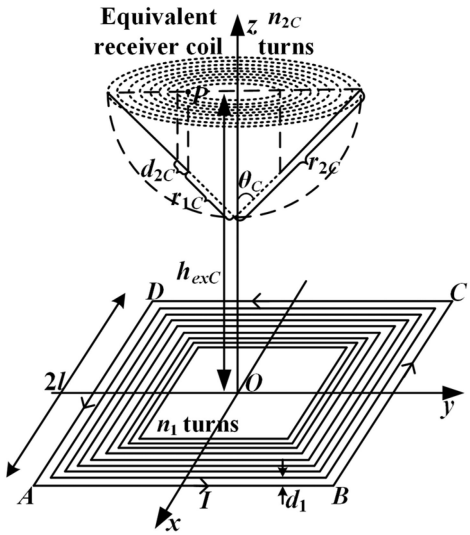

Fig. 5. Simplified model of the curved coil system.

TABLE II
TAPERED COIL SYSTEM PARAMETERS

Parameters	Transmitter coil	Receiving coil
Turns n_T	9	9
Turn spacing d_T/m	0.002	d_{2T}
Current I_T/A	5	I_R
Inner diameter $2r_T$/m	0.048	$2r_{1T}$

coil WPT system can be transformed into the magnetic flux expression of the curved coil WPT system as follows:

$$\begin{cases} \Psi_C = \Psi_T \\ r_{1T}\cos\theta_T + (n_{2T}-1)d_{2T}\cos\theta_T = 0 \\ r_{1C} = r_{1T}, d_{2C} = d_{2T} \\ r_{2C} = r_{2T}, \theta_C = \theta_T \\ n_{2C} = n_{2T}, h_{exC} = h_{exT}. \end{cases} \tag{5}$$

III. ANALYSIS OF THE TAPERED COIL WPT SYSTEM: TYPE-I

Based on modeling analysis and magnetic field calculation of the tapered coil WPT system presented in Section II-A, this section studies the influence of inner radius r_{1T} and turn spacing d_{2T} on the flux–cone angle curve under different transmission distances. The parameters of the transmitter coil and the tapered receiver coil are listed in Table II.

A. Influence of Inner Diameter on Magnetic Flux–Cone Angle Curve

Designing tapered coil turn spacing is 0.002 m, and five groups of data with an inner radius of 0.01–0.05 m are taken to analyze the changing trend of the magnetic flux passing through the tapered coil within the range of 0°–180°. Fig. 6 shows the magnetic flux–cone angle curves at the transmission distance h_{exT} of 0.01 m and 0.05 m, respectively.

It can be known from the figure that under a fixed transmission distance, with the increase in inner radius, the magnetic flux curve shows an overall upward trend, but when inner radius increases to a certain critical value, the peak value of the magnetic flux will decrease significantly. Taking Fig. 6(a) as an example, within inner radius of 0.01–0.03 m, the relationship between magnetic flux and cone angle is a single peak curve, but when the inner radius is greater than 0.04 m, the magnetic flux–cone angle curve has multiple extreme points, including one magnetic flux trough and peaks on both sides. Similar to the occurrence of frequency splitting when coils coupling coefficient is too large [19], [20], for a tapered coil WPT system, the phenomenon that the output power shows multiple peaks as cone angle changes under certain conditions is called angle splitting of tapered coil. Moreover, when the angle splitting does not occur, the cone angle corresponding to the curve's peak point also increases with the increase in inner diameter.

Comparing the curves of $r_{1T} = 0.05$ m in Fig. 6(a) and (b), it can be seen that the system changes from an angle-splitting state to an unsplit state with increasing distance. Therefore, when the transmission distance increases, the inner radius critical value r_{1Tc} without angle splitting also increases. In the application, it is possible to suppress the occurrence of angle splitting by reducing inner diameter of tapered coil and increasing transmission distance.

Fig. 7 shows the relationship between magnetic flux, cone angle, and inner radius at transmission distances of 0.01 m, 0.03 m, 0.05 m, and 0.07 m. In the figure, the magnetic flux peak value is marked with a triangle, and the magnetic flux valley value is marked with a circle.

It is easy to know that the larger inner diameter is, the easier it is to split, and the closer transmission distance is, the easier it is to split. There are one valley and two peaks in inner radius value where the angle split occurs, and both peaks are smaller than the single peak corresponding to inner radius critical value. For tapered coil applied to rockets and missiles, cone angle and required transmission distance can be obtained first. According to Fig. 7, inner radius corresponding to the optimal value of magnetic flux at a fixed angle can be selected to design coil, so as to improve transmission power of the tapered coil WPT system.

B. Influence of Turn Spacing on Magnetic Flux–Cone Angle Curve

As shown in Fig. 8, designing tapered coil inner radius is 0.02 m, and five groups of data with turn spacing of 0.001–0.005 m are taken to analyze the curve of magnetic flux varying as cone angle under transmission distance of 0.01 m and 0.05 m, respectively. When h_{exT} is 0.01 m, magnetic flux curve shows an overall upward trend with increase in turn spacing, but the curve peak will decrease when it increases to a certain critical value. Similarly, if turn spacing is too large, angle splitting would also occur. At the same time, as transmission distance increases, the curve ($d_{2T} = 0.005$ m) changes from splitting to unsplitting. Measures to reduce turn spacing and increase

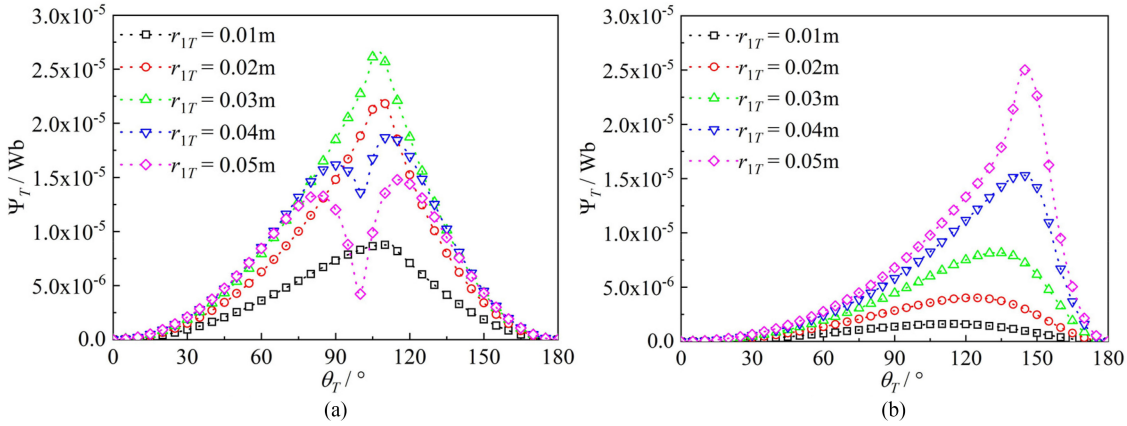

Fig. 6. Magnetic flux–taper angle curves under different inner diameters. (a) $h_{exT} = 0.01$ m. (b) $h_{exT} = 0.05$ m.

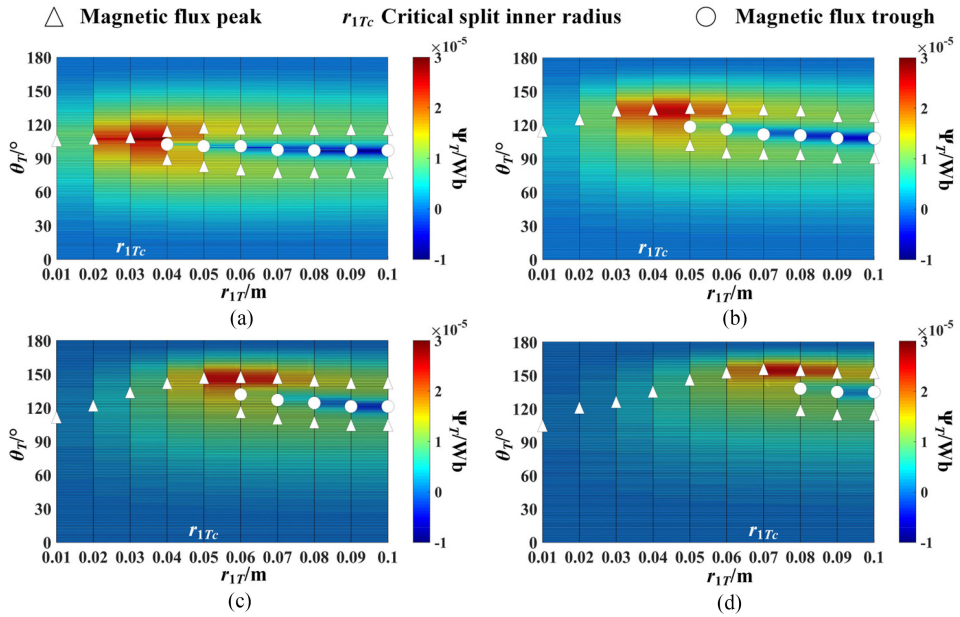

Fig. 7. Relationship between magnetic flux, taper angle, and inner radius at different transmission distances. (a) $h_{exT} = 0.01$ m (b) $h_{exT} = 0.03$ m. (c) $h_{exT} = 0.05$ m. (d) $h_{exT} = 0.07$ m.

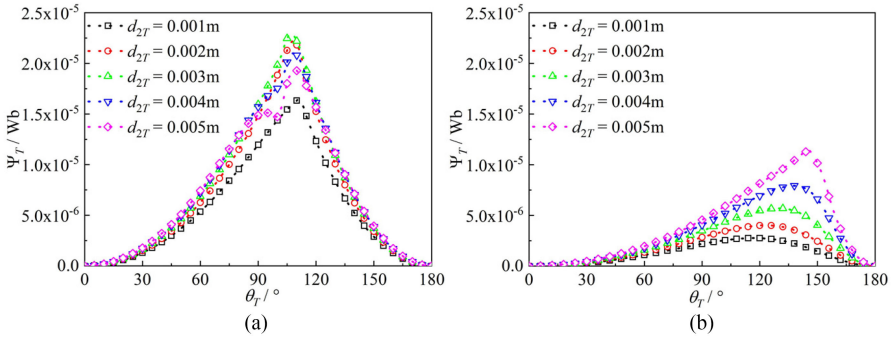

Fig. 8. Magnetic flux–taper angle curves under different turn spacings. (a) $h_{exT} = 0.01$ m. (b) $h_{exT} = 0.05$ m.

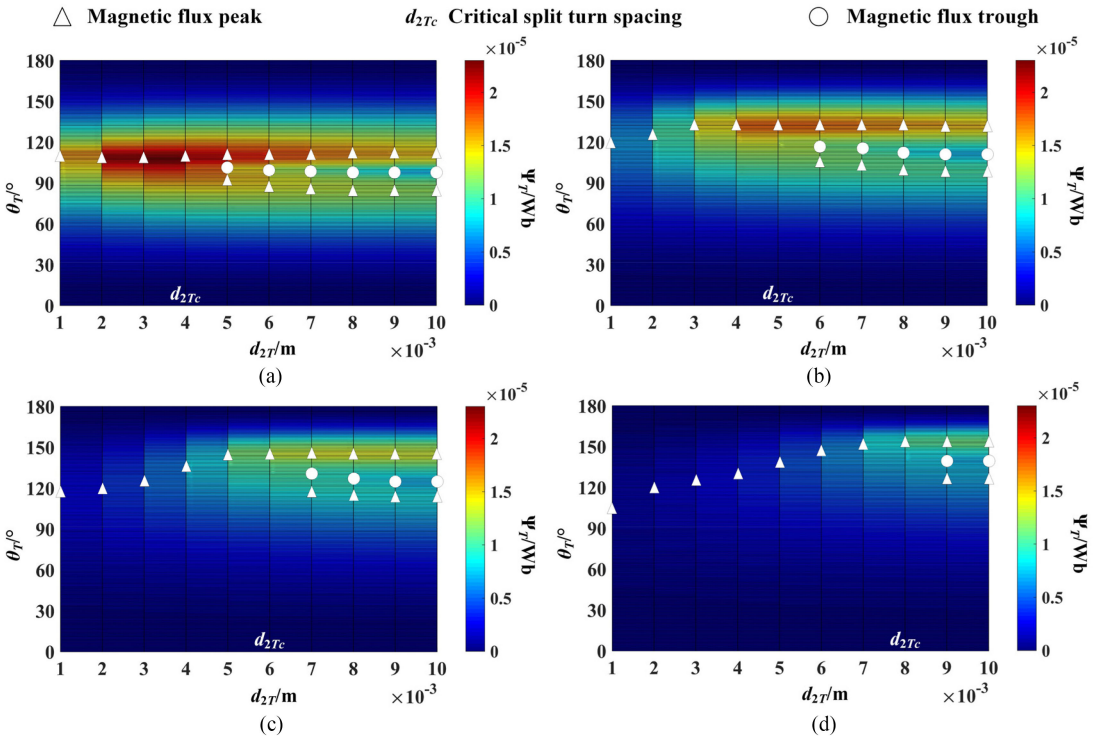

Fig. 9. Relationship between magnetic flux, taper angle, and turn spacing at different transmission distances. (a) $h_{exT} = 0.01$ m (b) $h_{exT} = 0.03$ m. (c) $h_{exT} = 0.05$ m. (d) $h_{exT} = 0.07$ m.

transmission distance can be taken to prevent the occurrence of angle splitting.

Fig. 9 shows the relationship between magnetic flux, cone angle, and turn spacing at transmission distances of 0.01 m, 0.03 m, 0.05 m, and 0.07 m. Using same mark as in Fig. 7, it can be seen that the larger the turn spacing is, the easier it is to split, and the closer the transmission distance is, the easier it is to split. Increasing transmission distance will also increase the critical value of turn spacing d_{2Tc}, and the splitting phenomenon caused by too large turn spacing also reduces the peak value of magnetic flux significantly. Therefore, in practical applications, the tapered coil can be designed by selecting turn spacing corresponding to the maximum magnetic flux at a certain cone angle and required transmission distance according to Fig. 9, so as to improve transmission power of the tapered coil WPT system.

In summary, we can conclude that the larger the inner diameter and turn spacing, the smaller the transmission distance, and the easier system is to split. Inner radius critical value r_{1Tc} and turn spacing critical value d_{2Tc} increase with the increase in the transmission distance. When there is no angle splitting, the cone angle of magnetic flux peak point increases with the increase in inner diameter and turn spacing.

IV. Analysis of the Curved Coil WPT System: Type-II

For the curved receiver coil WPT system, analyze the relationship between magnetic flux linkage Ψ_C passing through curved coil, curvature angle θ_C, and the parameters of the receiver coil, and study the relationship between magnetic flux change rate $\Delta\Psi_C$ and transmission distance h_{exC} under different parameters. Then, explore the system parameter design method based on the curved receiver coil to improve system's transmission performance. The default parameters of transmitter and receiver coils are shown in Table III.

TABLE III
Curved Coil System Parameters

Parameters	Transmitter coil	Curved receiver coil
Turns n	9	9
Turn spacing d/m	0.002	d_{2C}
Current I/A	5	I_R
Inner diameter $2r_1$/m	0.048	$2r_{1C}$
Transmission distance h_{exC}/m	0.05	

A. Curvature Angle Splitting

Similar to the tapered coil, for a WPT system with curved receiver coil, the phenomenon that output power presents multiple peaks as curvature angle changes under certain conditions is called the angle splitting or curvature angle splitting of curved coil. As shown in Fig. 10, under the circumstances that the receiver coil has a wide turn spacing, a large inner radius, or a small transmission distance, the magnetic flux of the curved coil exhibits two peaks as the curvature angle of receiver coil changes. Curvature angle splitting increases the complexity of

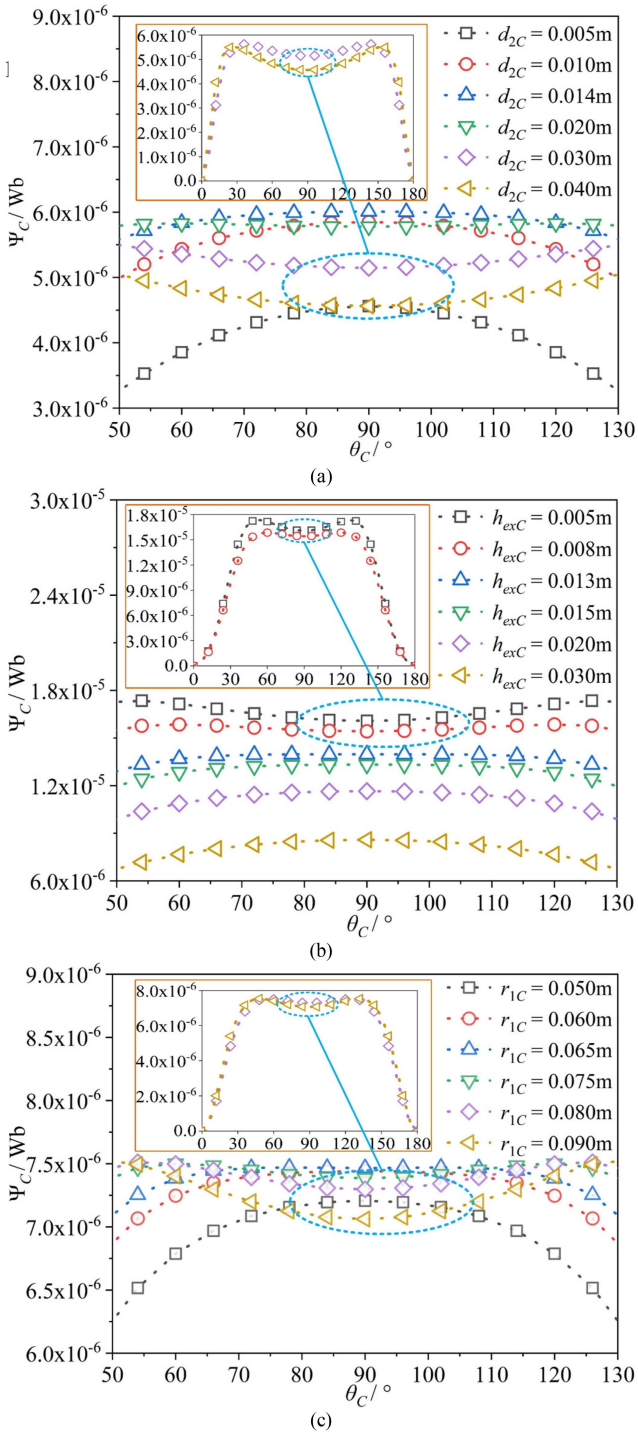

Fig. 10. Curvature angle splitting. (a) Curvature angle with d_{2C} splitting diagram when $h_{exC} = 0.05$ m and $r_{1C} = 0.02$ m. (b) Curvature angle with h_{exC} splitting diagram when $r_{1C} = 0.02$ m and $d_{2C} = 0.05$ m. (c) Curvature angle with r_{1C} splitting diagram when $d_{2C} = 0.005$ m and $h_{exC} = 0.05$ m.

system control and the instability of system, which has a great impact on transmission performance of the WPT system.

Fig. 10(a)–(c), respectively, shows three cases of curvature angle splitting under different turn spacings d_{2C} of the receiver coil, transmission distance h_{exC}, and radius r_{1C} of receiver coils. In Fig. 10(a), $h_{exC} = 0.05$ m and $r_{1C} = 0.02$ m, when $d_{2C} < 0.014$ m, magnetic flux Ψ_C follows a single-peak distribution with curvature angle θ_C, and Ψ_C reaches the maximum value when $\theta_C = 90°$, that is, receiver coil is not bent; when $d_{2C} = 0.014$ m, system is close to critical splitting state of curvature angle; when $d_{2C} > 0.014$ m, system has a curvature angle splitting, and two magnetic fluxes peak appear at symmetrical positions on both sides of $\theta_C = 90°$. In Fig. 10(b), $d_{2C} = 0.005$ m and $r_{1C} = 0.02$ m. When $h_{exC} < 0.013$ m, system has a curvature angle splitting, and the smaller the h_{exC}, the more obvious splitting phenomenon, but it will not cause a significant decrease in magnetic flux Ψ_C. In Fig. 10(c), $h_{exC} = 0.05$ m and $d_{2C} = 0.005$ m. Similar to Fig. 10(a), when $r_{1C} > 0.065$ m, system has a curvature angle splitting. In addition, it can be seen from Fig. 10 that when system is in a critical splitting state, magnetic flux can maintain good stability within a certain range of curvature angle change.

Through the abovementioned analysis, it can be known that the too small curvature angle splitting caused by transmission distance h_{exC} will not cause magnetic flux Ψ_C to drop significantly; the curvature angle splitting caused by receiver coil turn spacing d_{2C} or inner radius r_{1C} is too large, which will significantly reduce magnetic flux Ψ_C corresponding to θ_C in the range of 60°–120°, further resulting in a decrease in the received power. Therefore, measures need to be taken to suppress the occurrence of curvature angle splitting.

B. Mechanism and Suppression Method of Curvature Angle Splitting

According to the previous research and combined with the magnetic field characteristics of rectangular transmitter coil, it can be known that when the curvature angle $\theta_C = 90°$, that is, when receiver coil is not bent, its size has an optimal value related to the distance between the transmitter and receiver coils, so that received magnetic flux reaches maximum value. When the size of the curved receiver coil increases and exceeds the optimal value, received magnetic flux Ψ_C decreases instead, but during the bending process of the curved receiver coil, its equivalent receiver coil size changes with curvature angle. When the curvature angle deviates from 90°, the equivalent receiver coil gradually decreases, in this process, the equivalent receiver coil size will be exactly equal to the optimal size. Therefore, the magnetic flux Ψ_C will form peaks on both sides of curvature angle $\theta_C = 90°$ symmetry.

Since turn spacing d_{2C} and inner radius r_{1C} of the receiver coil in critical splitting state will change when transmission distance h_{exC} changes, the critical value of d_{2C} and the critical value of r_{1C} can be fitted respectively to guide coil parameter design so as to suppress curvature angle splitting.

In order to avoid curvature angle splitting caused by extensive values of d_{2C}, the critical values d_{2Cc} with respect to h_{exC} and r_{1C} are given in Fig. 11. In case the range of inner radius is 0.01–0.1 m and transmission distance is 0.01–0.1 m, the relationship expression of d_{2Cc}, h_{exC}, and r_{1C} is obtained by fitting, as

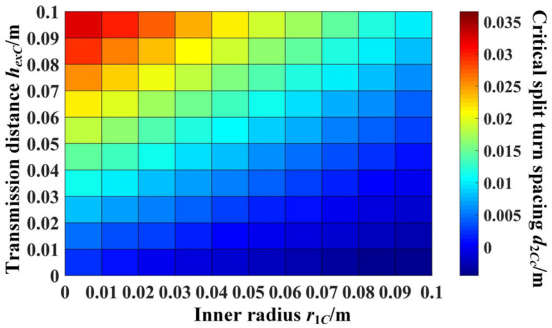

Fig. 11. Relationship between critical split turn spacing d_{2Cc} and h_{exC} and r_{1C}.

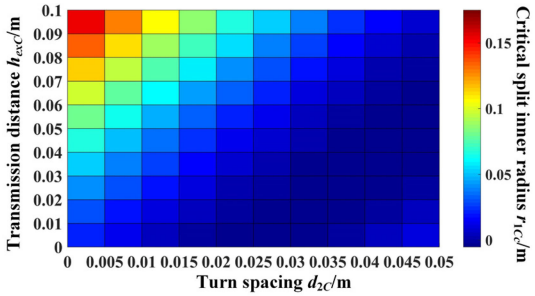

Fig. 12. Relationship between critical split inner radius r_{1Cc} and h_{exC} and d_{2C}.

shown in (6). The sum of squared errors (SSE) is 0.006804

$$d_{2Cc} = 0.4697r_{1C}^2 - 2.018r_{1C}h_{exC} + 0.4394h_{exC}^2 - 0.1117r_{1C} + 0.3009h_{exC} + 0.002067. \quad (6)$$

In order to avoid curvature angle splitting caused by extensive values of r_{1C}, the critical values r_{1Cc} with respect to h_{exC} and d_{2C} are given in Fig. 12. Within the turn spacing of 0.005–0.05 m and the transmission distance of 0.01–0.1 m, the relationship expression of r_{1Cc}, h_{exC}, and d_{2C} is obtained by fitting, as shown in (7). SSE is 0.004092.

$$r_{1Cc} = 41.36d_{2C}^2 - 33.34d_{2C}h_{exC} + 6.856h_{exC}^2 - 2.12d_{2C} + 0.8446h_{exC} + 0.02197. \quad (7)$$

We can first determine h_{exC}, r_{1C} or h_{exC}, d_{2C} according to actual application scenario and system requirements and then get d_{2Cc} or r_{1Cc} according to the fitted expression. In order to suppress the reduction of transmission power caused by curvature angle splitting, d_{2C} or r_{1C} needs to meet the following requirements:

$$d_{2C} \le d_{2Cc}$$
$$r_{1C} \le r_{1Cc}. \quad (8)$$

After comprehensive analysis of fitting results, it can be seen that receiver coils with small size and tightly wound are less prone to curvature angle splitting when bending. Moreover,

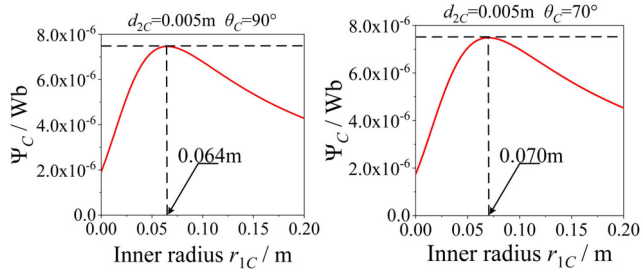

Fig. 13. Relationship between Ψ_C and r_{1C} when $d_{2C} = 0.005$.

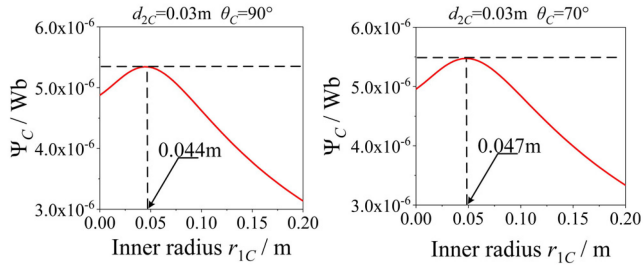

Fig. 14. Relationship between Ψ_C and r_{1C} when $d_{2C} = 0.03$ m.

when the system approaches critical splitting state of curvature angle, transmission power is maximized and stability is better.

C. Relationship Between Magnetic Flux and Receiver Coil Parameters

1) Relationship Between Magnetic Flux Ψ_C *and Receiver Coil Inner Radius* r_{1C}*:* It can be seen from Fig. 13 that receiver coil is tightly wound. When $\theta_C = 90°$ and $r_{1C} = 0.064$ m (not split) or θ_C =70° and, $r_{1C} = 0.07$ m (split), Ψ_C reaches the maximum. Fig. 14 illustrates that receiver coil is not closely wound. When $\theta_C = 90°$and $r_{1C} = 0.044$ m (split) or θ_C = 70°and $r_{1C} = 0.047$ m (split), Ψ_C reaches the maximum.

Comparing Figs. 13 and 14, when coil is not bent, that is, θ_C = 90°, the optimal outer diameter of receiver coil corresponding to $d_{2C} = 0.005$ m is $2 \times (r_{1C} + (n_{2C} - 1)d_{2C}) = 0.208$ m, and magnetic flux at this time is 7.46×10^{-6} Wb. However, the optimal outer diameter of receiver coil corresponding to d_{2C} = 0.03 m is 0.568 m, and at this time magnetic flux is 5.34×10^{-6}Wb. Although the former has a smaller coil size, it receives a larger magnetic flux, which still exists when $\theta_C = 70°$.

2) Relationship Between Magnetic Flux Ψ_C *and Receiver Coil Turn Spacing* d_{2C}*:* Let $r_{1C} = 0.02$ m, as shown in Fig. 15. When $\theta_C = 90°$ and $d_{2C} = 0.0135$ m (not split) or $\theta_C = 70°$ and $d_{2C} = 0.0148$ m (split), Ψ_C reaches its maximum.

To sum up, regardless of whether curvature angle is split or not, the receiver coil has an optimal inner diameter and turn spacing that maximizes received magnetic flux, and the greater the degree of coil bending, the greater the optimal values of inner diameter and turn spacing. Therefore, an optimal receiver coil can be designed according to degree of coil bending to ensure the maximum transmission power of system.

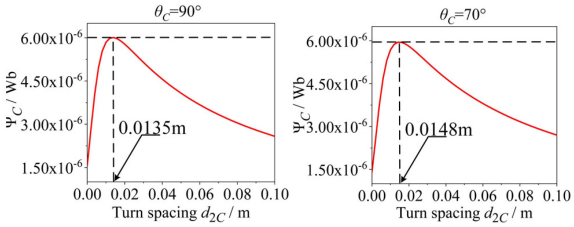

Fig. 15. Relationship between Ψ_C and d_{2C}.

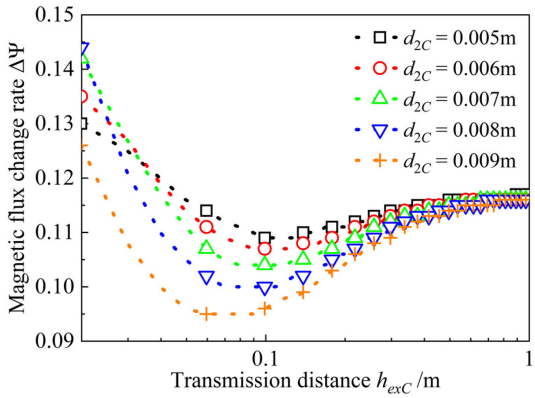

Fig. 16. Relationship between $\Delta\Psi$ and h_{exC} when $r_{1C} = 0.02$ m.

TABLE IV
MIN($\Delta\Psi$) AND CORRESPONDING h_{exC} UNDER DIFFERENT d_{2C}

d_{2C}/m	min($\Delta\Psi$)	h_{exC}/m
0.005	10.93%	0.0990
0.006	10.70%	0.0936
0.007	10.37%	0.0855
0.008	9.98%	0.0759
0.009	9.45%	0.0609

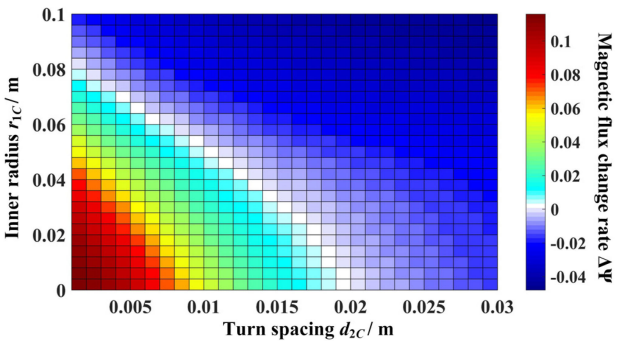

Fig. 17. Relation between $\Delta\Psi$ and d_{2C}, r_{1C}.

D. Relationship Between Magnetic Flux Change Rate and Transmission Distance

When curvature angle is not splitting, the bending of the receiver coil causes a reduction in magnetic flux passing through it; the magnetic flux change rate is defined as follows:

$$\Delta\Psi = \frac{\Psi_C\left(90^\circ, h_{exC}\right) - \Psi_C\left(70^\circ, h_{exC}\right)}{\Psi_C\left(90^\circ, h_{exC}\right)}. \tag{9}$$

Fig. 16 shows a graph of $\Delta\Psi$ and h_{exC} at five different turn spacings of receiver coil d_{2C} when $r_{1C} = 0.02$ m. Table IV shows the min ($\Delta\Psi$) and corresponding h_{exC} values under different d_{2C}. As can be seen from Table IV, on the premise, the curvature angle is not splitting, and min ($\Delta\Psi$) and its corresponding h_{exC} decrease as d_{2C} increases.

Therefore, the stability of wireless power transmission under different bending degrees can be effectively improved by reasonably adjusting the distance of transmitter and receiver coils.

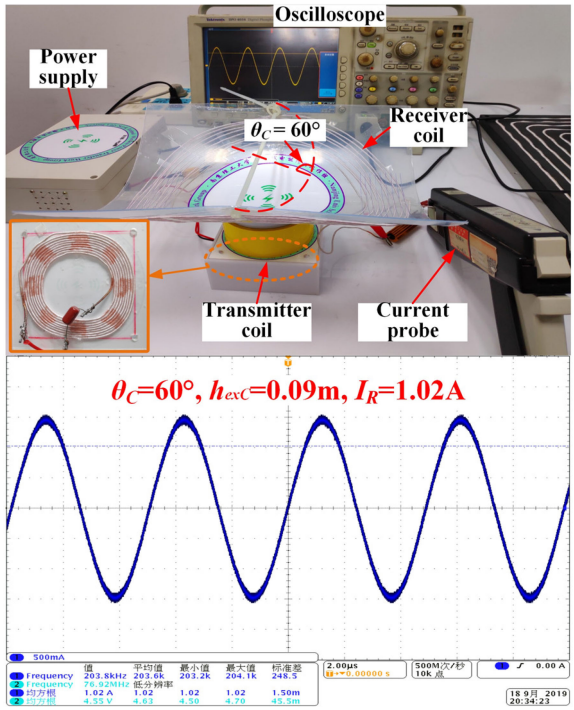

Fig. 18. Power stability experiment of curved coil wireless power transmission.

E. Relationship Between Magnetic Flux Change Rate and Parameters of Receiver Coil

It can be known from the previous studies that when system is in curvature angle critical splitting state, system's charging power can maintain better stability within a certain degree of bending of receiver coil.

Fig. 17 shows the relationship between magnetic flux change rate $\Delta\Psi$, turn spacing d_{2C}, and inner radius r_{1C} at a transmission distance of $h_{exC} = 0.05$ m. The magnetic flux change rate here is a function of d_{2C} and r_{1C}, that is

$$\Delta\Psi(d_{2C}, r_{1C}) = \frac{\Psi\left(90^\circ, d_{2C}, r_{1C}\right) - \Psi\left(70^\circ, d_{2C}, r_{1C}\right)}{\Psi\left(90^\circ, d_{2C}, r_{1C}\right)}. \tag{10}$$

The values of d_{2C} and r_{1C} can be restricted, as shown in Fig. 17. It can be found that when the parameters of receiver

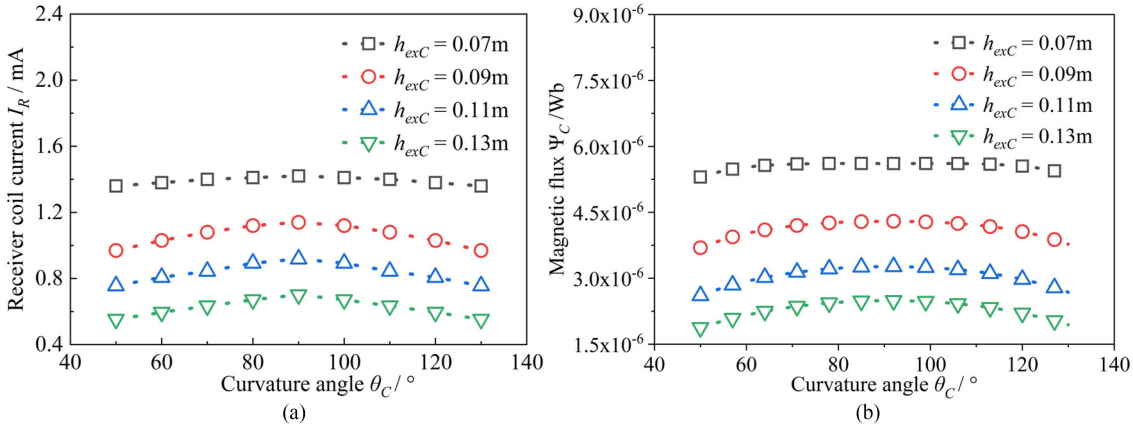

Fig. 19. Relationship between receiving coil current I_R and θ_C. (a) Experimental value. (b) Theoretical value.

TABLE V
EXPERIMENTAL PARAMETERS OF CURVED COIL WPT SYSTEM

Parameters	Transmitter coil	Receiver coil
Turns n	9	9
Turn spacing d/m	0.002	0.005
Inner diameter $2r$/m	0.048	0.18
Self-inductance L_s/μH	9.76	29.4
Compensation capacitance C_s/nF	68	22

TABLE VI
CURRENT CHANGE RATE AT DIFFERENT DISTANCES

h_{exC}/m	I_R/mA when θ_C=90°	I_R/mA when θ_C=70°	Current change rate ΔI_R
0.04	61.7	51.30	16.80%
0.06	39.4	33.30	15.50%
0.08	27.7	24.10	13.00%
0.10	20.9	16.50	21.05%
0.12	16.3	12.75	21.77%
0.14	12.3	9.57	22.16%

coil are close to critical splitting condition, magnetic flux change rate is within $\pm 2\%$. The wireless transmission power can be kept stable when curved coil is arbitrarily bent from 70° to 110°.

V. EXPERIMENTAL ANALYSIS

In this section, the relationship between system transmission performance and related parameters is experimentally validated.

A. Curvature Angle Critical Splitting and Analysis of System Power Stability

The traditional series compensation is adopted for the transmitter and receiver coils (SS). L_s and C_s represent the self-inductance of the coils and the corresponding compensation capacitance, respectively. The receiver coil is wound with litz wire and attached on a flexible polyvinyl chloride (PVC) board, and the load resistance is 3.3 Ω. Detailed experimental parameters of the transmitter and receiver coils are listed in Table V. Fig. 18 shows the experimental platform and waveforms. As the transfer distance $h_{exC} = 0.09$ m and the curvature angle $\theta_C = 60°$, the current picked up by the curved coil $I_R = 1.02$ A. When h_{exC} equals 0.07 m, 0.09 m, 0.11 m, and 0.13 m, the measured currents I_R as θ_C varies from 50° to 130° are shown in Fig. 19(a). Fig. 19(b) shows theoretical results of magnetic flux with respect to curvature angle. The trends of curves in Fig. 19(a) and (b) are coincident. The current rate of change is defined according to (9)

$$\Delta I_R = \frac{I_R\left(90°, h_{exC}\right) - I_R\left(70°, h_{exC}\right)}{I_R\left(90°, h_{exC}\right)}. \tag{11}$$

When $h_{exC} = 0.09$ m $I_R(\theta_C = 90°) = 1.16$ A, there is a single peak value in distribution of I_R versus θ_C. When $h_{exC} = 0.07$ m, the system is close to critical splitting state, I_R is almost unchanged at 1.40 A as θ_C varies from 50° to 130°, and the maximum current rate of change is 4.3%. Referring to the theoretical results concluded in Fig. 12 and (7), for the curved coil with parameters of $r_{1C} = 0.09$ m and $d_{2C} = 0.005$ m, when $h_{exC} = 0.072$ m, the system will close to critical splitting state, which is consistent with the experimental result of $h_{exC} = 0.07$ m.

We can conclude from the experimental results that the transfer power picked up by the curved receiver coil will be stabilized in a large degree of bend as the WPT system is modulate to critical splitting state, which will improve the adaptability of curved coil in different application scenarios.

B. Relationship Between the Current Rate of Change and the Transfer Distance

We change the experimental parameters of the system, i.e., inner radius to 0.02 m, self-inductance to 8.07 μH, and compensation capacitor to 100 nF, and the others are the same as listed in Table V. The currents picked up by curved receiver coil when $\theta_C = 90°$ (uncurved) and 70° under different transfer distance are measured. The results are listed in Table VI.

The experimental and theoretical results of the current rate of change are compared in Fig. 20. When $h_{exC} = 0.08$ m, ΔI_R achieves the minimum value of 13% in experiment, whereas the minimum value min($\Delta\Psi$) equals 10.93% when $h_{exC} = 0.099$ m

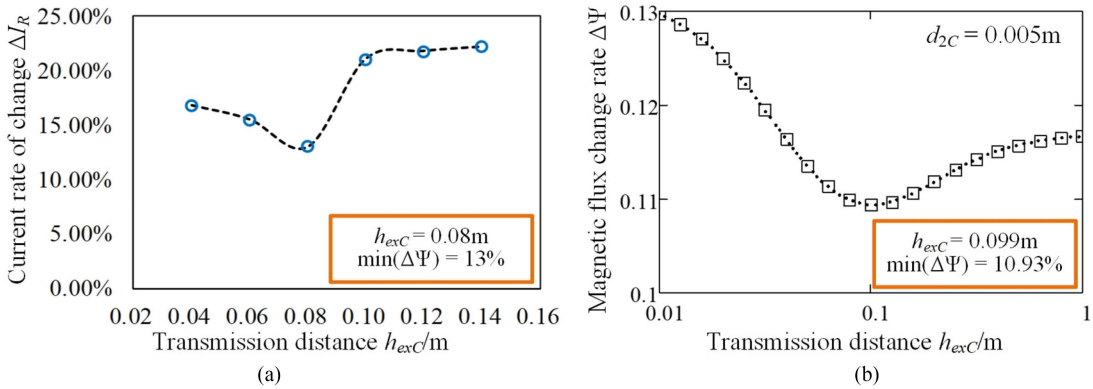

Fig. 20. Relationship between current change rate and transmission distance. (a) Experimental value. (b) Theoretical value.

in theoretical analysis. The errors can be caused by coil winding, and the experimental results still prove that when the curvature of the receiving coil changes, there exists an optimal value of transfer distance to achieve the lowest power fluctuation.

VI. Conclusion

In this article, the phenomenon of curvature angle splitting is investigated and a method is proposed to improve the transmission performance of the WPT system with tapered or curved receiver coil. By optimizing the coil parameters to make the system work in critical splitting state, the optimal output power and excellent stability under different angles are achieved. The proposed method is validated by experimental prototype. The experimental results show that the rate of change of the current picked up by the designed curved receiver coil is only 4.3% when the curvature angle is arbitrarily changed in the range of 50°–130°. Some other significant conclusions can be drawn as follows.

1) The mechanism of curvature angle splitting is revealed. Formulas are derived to determine the critical values of receiver coil radius and turn spacing. The receiver coils with small size and wound tightly are less prone to encounter the curvature angle splitting.
2) The curvature angle splitting can also be avoided by increasing the transmission distance. The stability of the WPT system can be effectively improved by rationally adjusting the transmission distance.

References

[1] K. B. S. Kiran, M. Kumari, R. K. Behera, O. Ojo, and A. Iqbal, "Analysis and experimental verification of three-coil inductive resonant coupled wireless power transfer system," in *Proc. Nat. Power Electron. Conf.*, Pune, India, 2017, pp. 84–89.

[2] B. J. Varghese, P. B. Bobba, and M. Kavitha, "Effects of coil misalignment in a four coil implantable wireless power transfer system," in *Proc. IEEE 7th Power India Int. Conf.*, Bikaner, India, 2016, pp. 1–6.

[3] K. Chen and Z. Zhao, "Analysis of the double-layer printed spiral coil for wireless power transfer," *IEEE J. Emerg. Sel. Top ics Power Electron.*, vol. 1, no. 2, pp. 114–121, Jun. 2013.

[4] R. Pinto, V. Lopresto, and A. Genovese, "A numerical study for the design of a new DD coil prototype for dynamic wireless charging of electric vehicles," in *Proc. 12th Eur. Conf. Antennas Propag.*, London, U.K., 2018, pp. 1–5.

[5] S. H. Lee, S. Lee, H. Song, and H. S. Lee, "Wireless sensor network design for tactical military applications: Remote large-scale environments," in *Proc IEEE Mil. Commun. Conf.*, Boston, MA, USA, 2009, pp. 1–7.

[6] M. Qiu, P. Jiang, Q. Chen, and Y. Jin, "Application study on prognostics and health management of armored equipment based on wireless sensor networks," in *Proc. Prognostics Syst. Health Manage. Conf.*, Zhangiiaijie, China, 2014, pp. 229–232.

[7] V. Bana, M. Kerber, G. Anderson, J. D. Rockway, and A. Phipps, "Underwater wireless power transfer for maritime applications," in *Proc. IEEE Wireless Power Transfer Conf.*, Boulder, CO, USA, 2015, pp. 1–4.

[8] B. Zhao, J. Wang, D. Sun, and H. Zhou, "Application of wireless transmission technology in weapon setting," in *Proc. 37th Chin. Control Conf.*, Wuhan, China, 2018, pp. 7262–7267.

[9] S. Jeong *et al.*, "Smartwatch strap wireless power transfer system with flexible PCB coil and shielding material," *IEEE Trans. Ind. Electron.*, vol. 66, no. 5, pp. 4054–4064, May 2019.

[10] S. Jeong *et al.*, "Design and analysis of wireless power transfer system using flexible coil and shielding material on smartwatch strap," in *Proc. IEEE Wireless Power Transfer Conf.*, Taipei, Taiwan, 2017, pp. 1–3.

[11] S. Jeong *et al.*, "Design, simulation and measurement of flexible PCB coils for wearable device wireless power transfer," in *Proc. IEEE Wireless Power Transfer Conf.*, Montreal, QC, Canada, 2018, pp. 1–4.

[12] G. Fotheringham, F. Ohnimus, I. Ndip, S. Guttowski, and H. Reichl, "Parameterization of bent coils on curved flexible surface substrates for RFID applications," in *Proc. 59th Electron. Compon. Technol. Conf.*, San Diego, CA, USA, 2009, pp. 502–507.

[13] S. Y. Y. Leung and D. C. C. Lam, "Performance of printed polymer-based RFID antenna on curvilinear surface," *IEEE Trans. Electron. Packag. Manuf.*, vol. 30, no. 3, pp. 200–205, Jul. 2007.

[14] J. Moon, S. Kim, S. Kim, and I. Cho, "Inductance calculation for the curved rectangular coil," in *Proc. Progress Electromagn. Res. Symp. - Fall*, Singapore, 2017, pp. 2650–2652.

[15] D. Zhu *et al.*, "Near field wireless power transfer using curved relay resonators for extended transfer distance," *J. Phys.: Conf. Series*, vol. 660, no. 1, 2015, Art. no. 012136.

[16] H. Gulzar, N. U. Ain, T. Zahid, M. F. Yaseen, A. Hussain, and S. A. Rahman Kashif, "A comprehensive electromagnetic design, simulation and analysis of wireless charging coils for large power applications," in *Proc. Prog. Electromagn. Res. Symp.*, Toyama, Japan, 2018, pp. 2476–2483.

[17] M. F. C. Jorgetto, G. D. A. E Melo, and C. A. Canesin, "Wireless inductive power transfer, oriented modeling and design," in *Proc. IEEE 13th Brazilian Power Electron. Conf. /1st Southern Power Electron. Conf.*, Fortaleza, Brazil, 2015, pp. 1–6.

[18] Y. Cheng and Y. Shu, "A new analytical calculation of the mutual inductance of the coaxial spiral rectangular coils," *IEEE Trans. Magn.*, vol. 50, no. 4, Apr. 2014, Art no. 7026806.

[19] F. Nasr, M. Madani and M. Niroomand, "Precise analysis of frequency splitting phenomenon of magnetically coupled wireless power transfer system," in *Proc. IEEE Asia Pac. Microw. Conf.*, Kuala Lumpar, Malaysia, 2017, pp. 219–224.

[20] D. Xu, S. Yin, and D. Wang, "Analysis of frequency splitting phenomena for magnetic resonance wireless power transfer systems," in *Proc. Chin. Automat. Congr.*, Jinan, China, 2017, pp. 2614–2618.

Feng Wen was born in Jiangsu, China, in 1990. He received the B.S. degree in electrical engineering and automation from the School of NARI Electric Automation, Nanjing Normal University, Nanjing, China, in 2011, and the Ph.D. degree in electrical engineering from the Southeast University, Nanjing, China, in 2017.

He is currently a Lecturer with the Nanjing University of Science and Technology, Nanjing, China. His current research interests include wireless power transfer, wireless charging for electric vehicles, and electromagnetic environments.

Fansheng Jing was born in Shandong, China, in 1996. He received the B.S. degree in electrical engineering and automation from the School of Information Science and Electrical Engineering, ShanDong JiaoTong University, Jinan, China, in 2018. He is currently working toward the M.S. degree with the Nanjing University of Science and Technology, Nanjing, China.

His current research interests include wireless power transfer for implantable medical devices and smart wearable devices.

Qiang Li received the B.S. degree in automatic control from the Harbin Institute of Technology, Harbin, China, in 1992, and the Ph.D. degree in electrical engineering from Southeast University, Nanjing, China, in 2005.

In 2005, he joined the School of Automation, Nanjing University of Science and Technology, Nanjing, China, where he has been engaged in teaching and research in the field of electrical engineering. His current research interests include electrical machine control and wireless power transfer.

Rui Li was born in Jiangsu, China, in 1995. He received the B.S. degree in electrical engineering and automation from the School of Electrical and Information Engineering, Jiangsu University, Zhenjiang, China, in 2017. He is currently working toward the M.S. degree with the Nanjing University of Science and Technology, Nanjing, China.

His current research interests include wireless power transfer for electric vehicles and electromagnetic filed shielding.

Li Liu was born in Jiangsu, China, in 1994. He received the B.S. degree in electrical engineering and automation in 2017 from the Nanjing University of Science and Technology, Nanjing, China, where he is currently working toward the M.S. degree in electrical engineering.

His current research interest includes wireless power transfer.

Xiaohu Chu was born in Anhui, China, in 1994. He received the B.S. degree in maritime electrical and electronic engineering from Dalian Maritime University, Dalian, China, in 2017. He is currently working toward the M.S. degree with the Nanjing University of Science and Technology, Nanjing, China.

His current research interests include wireless power transfer for implantable medical devices and smart wearable devices.